

# Ultrathin Free-Standing Polyelectrolyte Nanocomposites: A Novel Method for Preparation and Characterization of Assembly Dynamics

James K. Ferri,<sup>\*,†,‡</sup> Wen-Fei Dong,<sup>‡</sup> and Reinhard Miller<sup>‡</sup>

*Department of Chemical Engineering, Lafayette College, Easton, Pennsylvania 18042, Max Planck Institute of Colloids and Interfaces, Golm/Potsdam, D-14476, Germany*

*Received: May 21, 2005; In Final Form: July 5, 2005*

We present a new opportunity for the investigation of the dynamics of electrostatic ultrathin-film assembly and the elucidation of time scales required for layer-by-layer adsorption of polyelectrolytes using a novel pendant drop technique which allows for the synthesis of free-standing nanocomposites. In short, a charged molecular template, i.e., a lipid monolayer, is deposited on a pendant drop and compressed to present a defined surface charge density to the subphase of the drop. The subphase is then cycled alternatively between solutions of polycations, saline, and polyanions by injection and withdrawal of liquid from coaxial capillaries on which the drop was formed, resulting in encapsulation of the drop volume by a polymeric composite membrane. The in situ dynamics of the process are followed by axisymmetric drop shape analysis. As a model, nanocomposites of dimyristoyl phosphatidyl glycerol-(polyallylamine hydrochloride/polystyrene sulfonate)<sub>*n*=1–3</sub> were prepared. The characteristic time scales for assembly range from 1 to 4 min and increase with film thickness. It is also demonstrated that small-amplitude (>1%) perturbations in the film density during adsorption prolong the assembly. Both these results underscore the nonequilibrium nature of these materials.

## Introduction

The electrostatic layer-by-layer (LbL) assembly of materials into ultrathin films has developed as a promising technique for the modification of a wide variety of surfaces and interfaces because of its facility and versatility.<sup>1,2</sup> Although much attention has been given to the development of new materials,<sup>3,4</sup> their structure,<sup>5,6</sup> and new applications, the kinetics of the assembly process at the interface are not well-understood, in part due to the lack of suitable experimental methodology.<sup>7</sup> Therefore, it is necessary to seek a simple and efficient technique to measure the assembly of the LbL process in order to understand the in situ dynamics in these thin films.

During the past decade, axisymmetric drop shape analysis (ADSA) has emerged as a powerful tool for the study of interfacial dynamics and has been successfully used to study surfactant adsorption kinetics<sup>8,9</sup> and the interfacial rheology of a variety of single<sup>10</sup> and multicomponent<sup>11,12</sup> systems at fluid interfaces. However, to the best of our knowledge, ADSA has not been used to study the assembly of LbL nanocomposites.

In this letter, we report for the first time a strategy for the preparation and characterization of free-standing ultrathin nanocomposite films using layer-by-layer adsorption of polyelectrolytes onto a charged insoluble monolayer template at the aqueous/air interface of a single pendant drop. The importance of this technique is that the geometry of the drop interface

permits highly precise measurement of the dynamic surface tension and therefore the evolution of the surface free energy during synthesis, providing insight into the dynamics of polyelectrolyte assembly inaccessible by other methods. We also report results of the influence of the template surface charge density on the kinetics, which despite the overwhelming number of studies in LbL synthesis has not been studied systematically.

## Experimental Section

The foundation of the experimental setup is a commercially available pendant drop tensiometer (Sinterface Technologies, Germany). A schematic of the apparatus is shown in Figure 1a. In short, a silhouette of a pendant drop formed at the tip of a capillary is cast onto a CCD camera and digitized. A specially constructed capillary consisting of a concentric geometry fabricated from glass microtubing and poly(ether ether ketone) (PEEK) was used for drop formation. This geometry allows a drop of aqueous solution to be formed at the capillary tip and the subphase to be exchanged by injection (from syringe pump 2) and withdrawal (from syringe pump 1) of liquid from the droplet interior at a matched volumetric flow rate ( $R_E$ ). During the exchange, the interfacial area of the drop is maintained constant by feedback control using syringe pump 1. A more detailed discussion of the subphase exchange has been presented previously.<sup>11,12</sup> The digital images of the drop are recorded over time and fit to the Young–Laplace equation to accurately  $\pm 0.1$  mN/m determine surface tension. Further details of axisymmetric drop shape analysis are described in detail elsewhere.<sup>13</sup>

\* To whom correspondence should be addressed: ferrij@lafayette.edu.

<sup>†</sup> Lafayette College.

<sup>‡</sup> Max Planck Institute of Colloids and Interfaces.

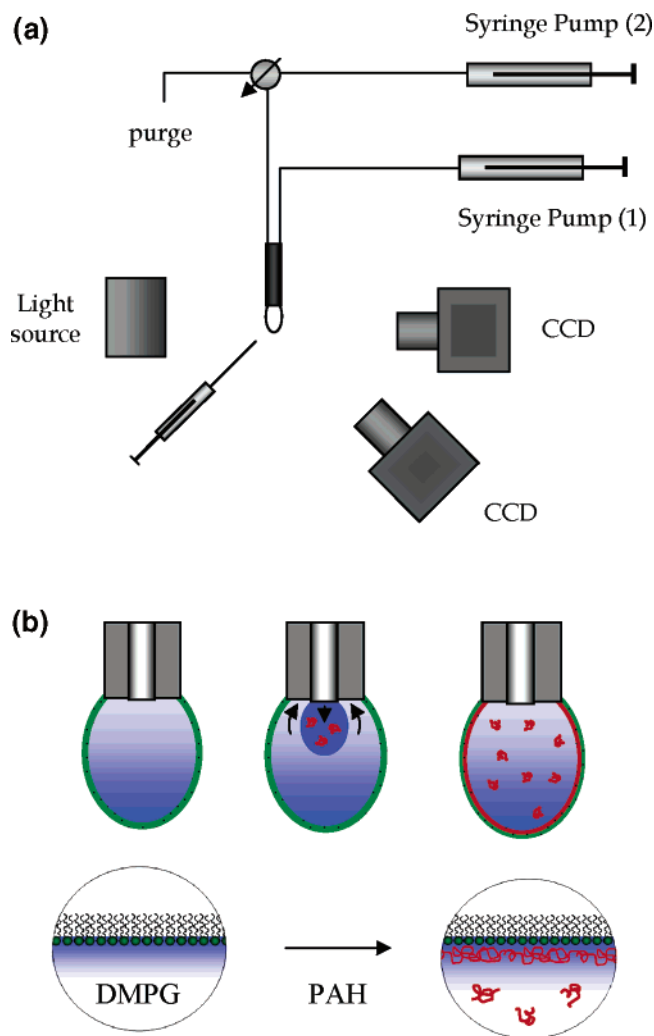


**Figure 1.** Layer-by-layer synthesis of free-standing films. (a) Schematic of pendant drop coaxial capillary setup. (b) Schematic of layer-by-layer templating on a lipid monolayer at the free surface.

Figure 1b shows a scheme for the preparation of a free-standing nanocomposite using the setup described above. First, an insoluble monolayer is deposited onto a pendant drop of aqueous saline solution and compressed. The subphase of the drop is then exchanged, maintaining constant surface area with a subphase containing a polyelectrolyte (PE) of opposite charge to the template. Alternate cycles of cationic and anionic polyelectrolyte and intermittent flushing result in free-standing polymeric nanocomposites having a thickness which is defined by the number of adsorption layers.<sup>14</sup> Exchange flow rate ( $R_E \approx 1 \mu\text{L/s}$ ) and total interfacial area of the drop ( $A_D = 25.3 \pm 0.3 \text{ mm}^2$ ) during exchange as well as template density are controlled. The pH is approximately 7.0 in all experiments.

Results are presented using dimyristoyl phosphatidyl glycerol (DMPG) as a template for the well-studied model polyanion–polycation pair of poly(styrene sulfonate) sodium salt (PSS,  $M_w \approx 70 \text{ kDa}$ ) and poly(allylamine hydrochloride) (PAH,  $M_w \approx 70 \text{ kDa}$ ). Sodium chloride is a buffer for ionic strength. All materials were purchased from Aldrich, and the structures are given in the Supporting Information. All chemicals were used as received except for PSS, which was dialyzed before use ( $M_w 50 \text{ kDa}$  cutoff). Lipid spreading solutions were prepared with ultrapure chloroform and methanol, approximately (3:1 v/v) from J. T. Baker. Polyelectrolyte solutions were  $C_P = 1 \text{ mM}$  monomer. In both polyelectrolyte and flushing solutions, the salt concentration was  $0.25 \text{ M NaCl}$ . The water used for all

solutions was purified in a three-stage Milli-Q Plus 185 purification system and had a resistivity higher than  $18.2 \text{ M}\Omega/\text{cm}$ . Lipid monolayers were spread onto the drop by microsyringe (Hamilton, U.S.A.) using (x, y, z) positioning stages from a spreading solution of concentration approximately ( $0.25 \text{ mg/mL}$ ) in chloroform/methanol (3:1 v/v). A typical drop ( $V_D = 17 \mu\text{L}$ ) requires approximately  $V = 0.25 \mu\text{L}$  to deposit a monolayer of approximately  $1/\Gamma = 100 \text{ \AA}^2/\text{molecule}$ . The deposition is monitored using a second CCD camera to image the contact between the microsyringe and droplet in parallel, and approximately 10 min are allowed for solvent evaporation prior to further experiments. Resultant films in this study are of the structure  $\text{DMPG-(PAH/PSS)}_n$ , where  $n$  is the number of bilayer pairs.

## Results and Discussion

The use of molecular monolayers as templates for the synthesis and characterization of polyelectrolyte multilayer nanocomposites is attractive, because the charge density of the interface can be precisely controlled without changing the chemical composition of the template. The lipid (DMPG) used in this study forms a stable monolayer with no surface phase transitions. Furthermore, a high degree of dissociation ( $<90\%$ ) has been reported for a similar lipid (DMPA)<sup>15</sup> on a saline subphase for surface densities between  $40 < 1/\Gamma < 120 \text{ \AA}^2/\text{molecule}$ . Thus, surface charge density of the template can be assumed a spatially uniform and linear function of surface density.

The free energy changes in the monolayer provide information on the dynamics of structure formation in the polymeric composite. Figure 2a–c shows a typical trace of the surface tension,  $\gamma$ , during the synthesis of a six-layer composite, i.e.,  $n = 3$ . The presence of the composite at the interface was confirmed by collection of the droplet in aqueous solution and confocal imaging of the free-standing film in solution; see the Supporting Information for images. As seen in Figure 2a, the change in surface tension is most dramatic upon the adsorption of the first polyelectrolyte monolayer, which can be understood as a result of the screening of Coulombic repulsion of the charged lipid headgroups due to the binding of the polymeric counterion that lowers the surface pressure (or increases the surface tension.). This electrostatic contribution of the surface tension has been calculated on the basis of the Guoy–Chapman theory and amounts to approximately  $9 \text{ mN/m}$ .<sup>15</sup> Although theory dictates that changes in the surface tension have the opposite sign to changes in the surface potential, the data in Figure 2a indicate that the surface potential decreases upon adsorption of each of the first two layers and alternates (as expected) only for subsequent layers. Further experiments involving direct, in situ measurement of the surface potential are required to confirm this phenomenon.

The dynamics of the adsorption can be modeled by a mass balance at the interface, in which the rate of adsorption is proportional to the concentration of polyelectrolyte adjacent to the interface,  $C_s$ , and the number of free adsorption sites ( $\Gamma_{\text{max}} - \Gamma$ ), and the rate of desorption is proportional to the amount of adsorbed polymer ( $\Gamma$ )

$$\frac{\partial \Gamma}{\partial t} = \beta C_s (\Gamma_{\text{max}} - \Gamma) - \alpha \Gamma \quad (1)$$

where  $\Gamma$  is the surface density of adsorbed polyelectrolyte, and  $\beta$  and  $\alpha$  are the rate constants of adsorption and desorption, respectively. The exchange of the subphase introduces a convective supply of polyelectrolyte to the interface so that the

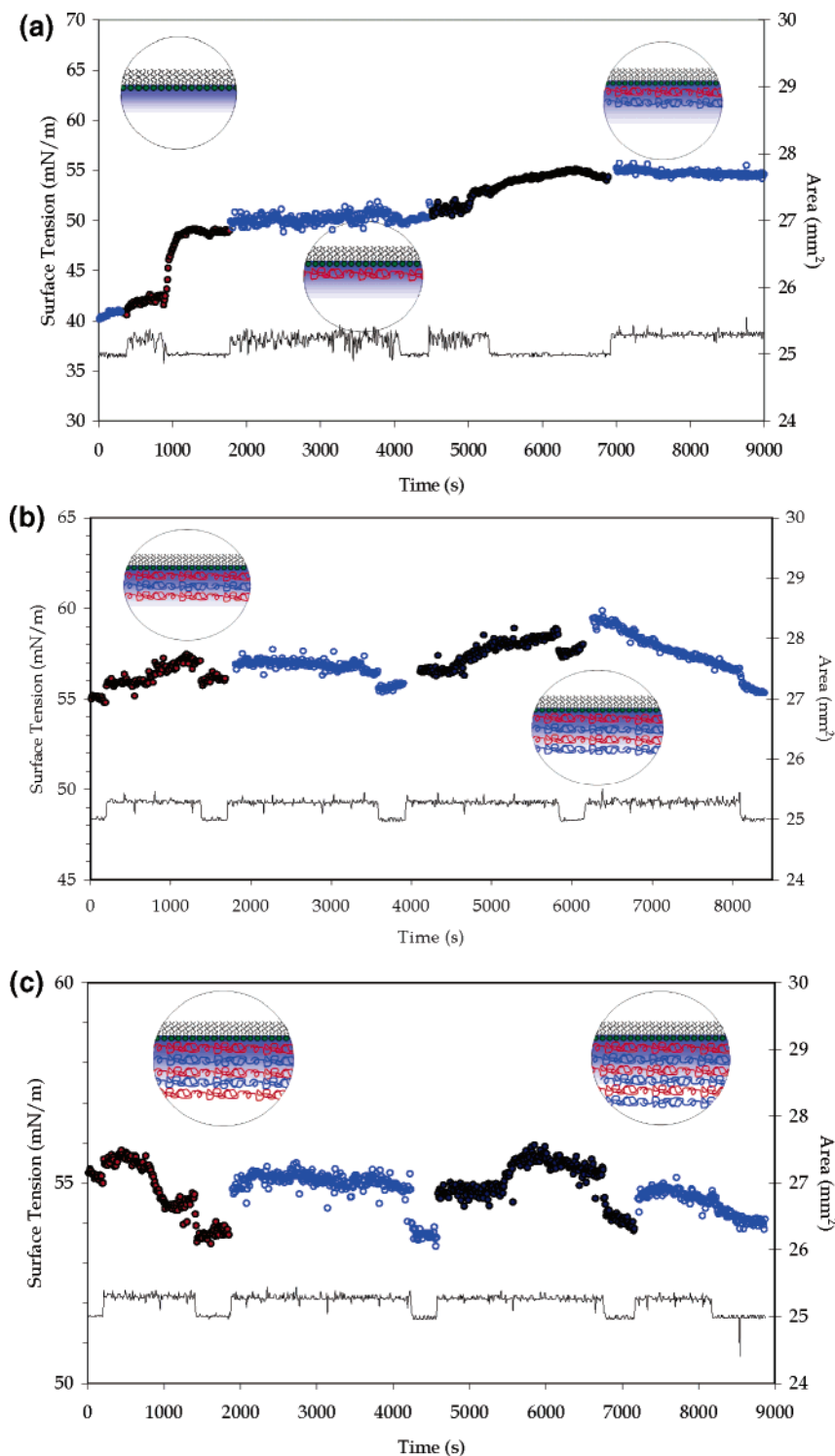


**Figure 2.** Synthesis of a DMPG-(PAH/PSS)<sub>n=3</sub> free-standing nanocomposite. Dynamic trace of surface tension (symbols) and total interfacial drop area (line) vs time for (a) DMPG-PAH (red), DMPG-PAH/NaCl flush (light blue), DMPG-PAH/NaCl flush/PSS (dark blue), DMPG-PAH/NaCl flush/PSS/NaCl flush (light blue), (b) DMPG-(PAH/PSS)<sub>n=1</sub> to DMPG-(PAH/PSS)<sub>n=2</sub>, and (c) DMPG-(PAH/PSS)<sub>n=2</sub> to DMPG-(PAH/PSS)<sub>n=3</sub>.

concentration of polymer adjacent to the surface,  $C_s$ , is approximately constant during adsorption, so that the solution of eq 2 is

$$\Gamma(t) = \frac{\beta C_s \Gamma_{\max}}{\beta C_s + \alpha} \{1 - \exp[-(\beta C_s + \alpha)t]\} \quad (2)$$

Equation 2 can be rewritten

$$\theta_{\Gamma}(t) = 1 - \exp(-t/t_c) \quad (3)$$

where  $\theta_{\Gamma} = \Gamma/\Gamma_{\text{eq}}$  is the fraction of the equilibrium adsorbed amount in the Langmuir equilibrium adsorption framework and the characteristic adsorption time,  $t_c = (\beta C_s + \alpha)^{-1}$ . By rescaling the surface tension  $\theta_{\gamma} = (\gamma - \gamma_i)/(\gamma_{\text{eq}} - \gamma_i)$  and the assumption of local state, i.e., the adsorbed amount is reflected instantaneously in the surface tension, the characteristic time scale of the adsorption kinetics,  $t_c$ , can be calculated. Figure 3 shows the rate for the adsorption,  $\theta_{\gamma}$ , of the first polyelectrolyte layer (PAH) onto the template (DMPG) as a function of the surface pressure and therefore charge density of the template: 38, 40,

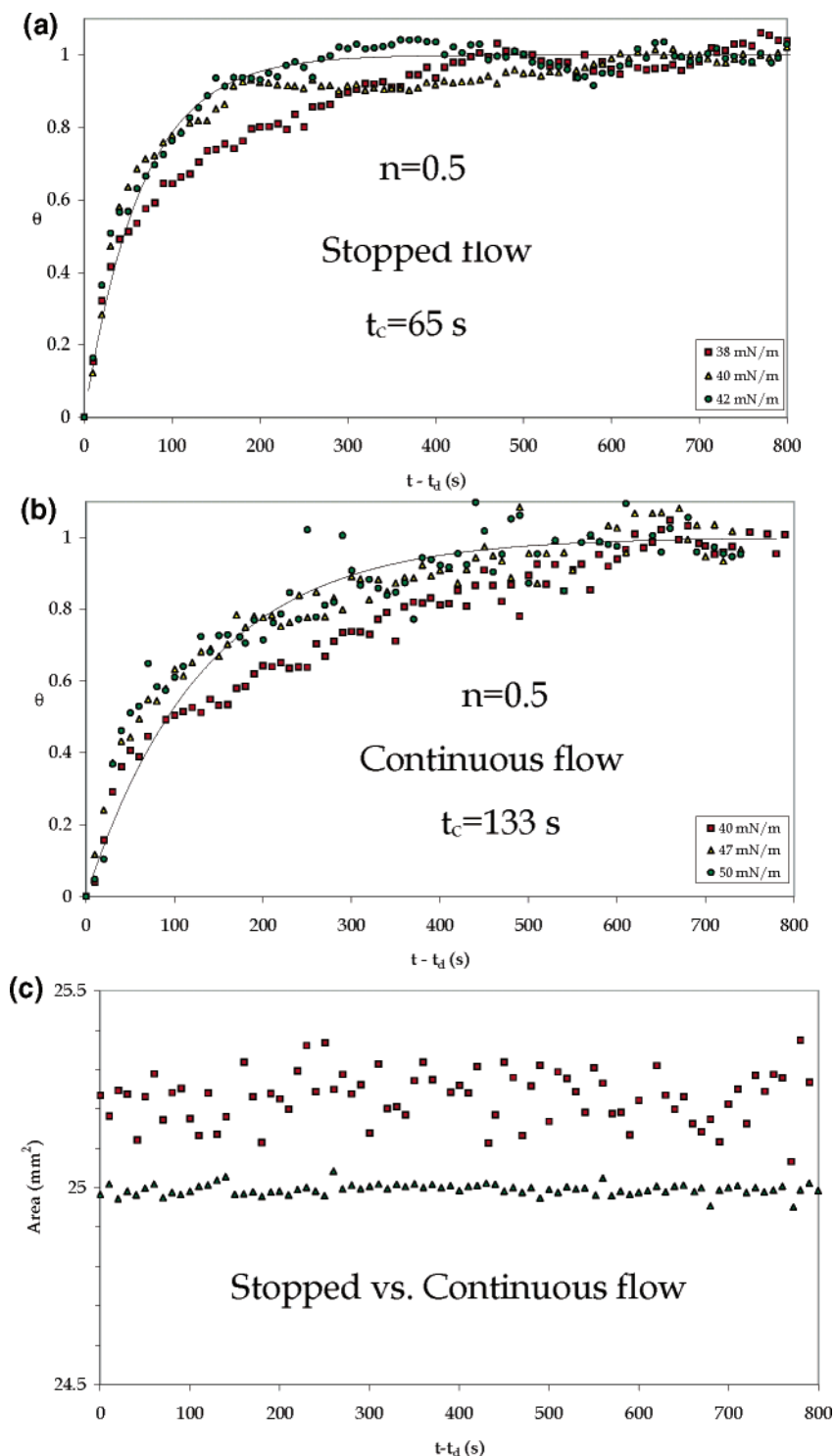


**Figure 3.** Dynamics of polyelectrolyte adsorption. Scaled surface tension  $\theta_\gamma$  vs time as a function of template density for (a) stopped flow, (b) continuous flow (solid line is best fit kinetic model fit), and (c) the drop area vs time for both stopped (triangles) and continuous (squares) flow.

and 42 mN/m in Figure 3a and 40, 47, and 50 mN/m in Figure 3b. Because the data nearly superimpose in the figure, it can be concluded that the kinetics of the assembly are relatively insensitive to surface charge density of the template. (The solid line shown in Figure 3a,b is the best fit of the kinetically controlled assembly model.) There is, however, one important condition which gives rise to the difference between the data in Figure 3a and b. The data in Figure 3a were obtained by exchanging the subphase until an increase in surface tension (indicating the presence of PE) was evident, and thereafter stopping the flow and allowing the adsorption to proceed without

further exchange, whereas in Figure 3b, the exchange was maintained continuously throughout the adsorption process. Although the increase in surface tension is approximately the same ( $9 \pm 0.5$  mN/m) in both cases, the interfacial area is nearly constant in Figure 3a and oscillatory in Figure 3b (albeit the amplitude is less than 1%). These oscillations in the surface area have a dramatic impact on the characteristic adsorption time, doubling  $t_c$  from 65 to 133 s. Two conclusions can be made: first, adsorption at constant interfacial area is relatively rapid for the first layer, in fact, much faster than the typical time allowed for layer-by-layer adsorption;<sup>1</sup> and second, com-

parison of the time scales in both experiments underscores the nonequilibrium nature of the PE structure, because small perturbations in the template area lead to rearrangement in the surface. Similar findings have been observed in simulation.<sup>16</sup> The characteristic time scale for the second layer, i.e., PSS onto DMPG-PAH, was also measured under continuous-flow conditions ( $t_c = 235$  s); see data in the Supporting Information. Because of the large disparity of the time scales for the first and second layers, rearrangement between PAH and DMPG upon the adsorption PSS is likely to occur.

## Conclusions

In this letter, a novel experimental framework was presented for the synthesis and study of ultrathin free-standing nanocomposites. Free-standing nanocomposites of the structure DMPG-(PAH/PSS)<sub>n=1-3</sub> were prepared on the surface of a pendant drop by precise subphase exchange and the dynamics of the synthesis were followed via in situ surface tension measurement. By variation of the density of the template, the effect of electrostatic charge density, and the film thickness on the dynamics of formation was probed. Using an adsorption-limited transport model, the characteristic time scale for assembly,  $t_c$ , was calculated using data of the time evolution of the surface tension during the adsorption of the PAH onto DMPG. The data underscore the nonequilibrium structure of the composite and suggest that the assembly time for one layer is between 1 and 4 min.

**Acknowledgment.** J.K.F. thanks the Alexander von Humboldt Foundation for support in the form of a Research Fellowship.

**Supporting Information Available:** The structure of the molecules forming the composite, confocal micrographs of the nanocomposite, and data showing the time evolution of the surface tension during adsorption of the second layer are given as Supporting Information. This material is available free of charge via the Internet at <http://pubs.acs.org>.

## References and Notes

- (1) Decher, G. *Science* **1997**, 277, 1232.
- (2) Hammond, P. T. *Curr. Opin. Colloid Interface Sci.* **1999**, 4, 430.
- (3) Bertrand, P.; Jonas, A.; Laschewsky, A.; Legras, R. *Macromol. Rapid Commun.* **2000**, 21, 319.
- (4) Jiang, C. Y.; Markutsya, S.; Tsukruk, V. V. *Adv. Mater.* **2004**, 16, 157.
- (5) Arys, X.; Laschewsky, A.; Jonas, A. M. *Macromolecules* **2001**, 34, 3318.
- (6) Dong, W. F.; Ferri, J. K.; Adalsteinsson, T.; Schonhoff, M.; Sukhorukov, G. B.; Mohwald, H. *Chem. Mater.* **2005**, 17, 2603.
- (7) Schonhoff, M. *J. Phys.: Condens. Matter* **2003**, 15, R1781.
- (8) Ferri, J. K.; Stebe, K. J. *Colloids Surf., A* **1999**, 156, 567.
- (9) Ferri, J. K.; Stebe, K. J. *Adv. Colloid Interface Sci.* **2000**, 85, 61.
- (10) Miller, R.; Fainerman, V. B.; Leser, M. E.; Michel, M. *Curr. Opin. Colloid Interface Sci.* **2004**, 9, 350.
- (11) Wege, H. A.; Holgado-Terriza, J. A.; Cabrerizo-Vilchez, M. A. *J. Colloid Interface Sci.* **2002**, 249, 263.
- (12) Ferri, J. K.; Miller, R.; Makievski, A. V. *Colloids Surf., A* **2005**, 261, 39.
- (13) Loglio, G.; Pandolfini, P.; Miller, R.; Makievski, A. V.; Ravera, F.; Ferrari, M.; Liggieri, L. Novel Methods to Study Interfacial Layers. In *Studies in Interface Science*; Möbius, D., Miller, R., Eds.; Elsevier: 2001; Vol. 11, p 439.
- (14) Ruths, J.; Essler, F.; Decher, G.; Riegler, H. *Langmuir* **2000**, 16, 8871.
- (15) Helm, C. A.; Laxhuber, L.; Losche, M.; Mohwald, H. *Colloid Polym. Sci.* **1986**, 264, 46.
- (16) Panchagnula, V.; Jeon, J.; Dobrynin, A. V. *Phys. Rev. Lett.* **2004**, 93.